Hindawi

Research Article

Investigation of the Efficiency of Roll Profiles and Technological Schemes of Deformation of Asymmetric Rolling in Relief Rolls of C11000 Copper Alloy by FEM Simulation

Evgeniy Panin [iD],[1] **Aibol Esbolat,**[1] **Alexandr Arbuz,**[2] **Dmitry Kuis,**[3] **Abdrakhman Naizabekov,**[4] **Sergey Lezhnev,**[4] **Almas Yerzhanov,**[1] **Ivan Krupenkin,**[1] **Andrey Tolkushkin,**[5] **Anna Kawalek,**[6] **and Pavel Tsyba**[7]

[1]*Karaganda Industrial University, 30 Republic Ave., Temirtau 101400, Kazakhstan*
[2]*AEO Nazarbayev University, 53 Kabanbay Batyr Ave., Astana 010000, Kazakhstan*
[3]*Belarusian State Technological University, 13a Sverdlova Str., Minsk 220006, Belarus*
[4]*Rudny Industrial Institute, 50 let Oktyabrya Str. 38, Rudny 111500, Kazakhstan*
[5]*Ural Federal University, 19 Mira Str., Yekaterinburg 620002, Russia*
[6]*Częstochowa University of Technology, 69 J.H. Dąbrowskiego Str., Częstochowa 42-201, Poland*
[7]*LLP "Promtech Perspective", 7/2 Prigorodnaya Str., Karaganda 100000, Kazakhstan*

Correspondence should be addressed to Evgeniy Panin; ye.panin@tttu.edu.kz

In this paper, finite element simulation of asymmetric rolling in relief rolls of C11000 copper alloy in order to analyze the effectiveness of possible roll profiles and technological schemes of deformation was performed. The scientific innovation of this work lies in determining the patterns of development of stress-strain state parameters for various configurations of rolls, as well as determining the effectiveness of metal processing using various technological schemes. It was found that the use of trapezoidal relief makes it possible to increase the level of metal processing by almost 5 times compared with the use of radial relief. Comparison of technological schemes of deformation showed that deformation with 180° workpiece turning between passes significantly reduces the influence of the asymmetry factor. Deformation without changing the workpiece position between the passes has the opposite effect, and such a scheme significantly increases the influence of the asymmetry factor. Deformation with a transverse workpiece shift for the relief period between passes has the effect of a "golden mean." The conducted laboratory experiment for lead billet showed that the shape change of lead billet during computer simulation has a high level of convergence with real conditions. At each stage of deformation, the difference in the geometric parameters of the workpiece between the model and the experiment did not exceed 3-5%. When deforming a copper billet, the maximum difference level was 8%, which is the result of the low rigidity of the rolling cage with smooth rolls.

1. Introduction

Scientific works on obtaining high-quality metal with various methods of severe plastic deformation (SPD) are among the most cited publications in the world [1–3]. The SPD implementation due to the intensification of shear and alternating strains makes it possible to achieve the refinement of the initial structure to an ultrafine-grained state and obtain unique mechanical characteristics, which are sometimes par-adoxical [4, 5]. At the same time, the most well-known SPD methods—high-pressure torsion (HPT) and equal-channel angular pressing (ECAP)—allow deforming samples of limited geometric dimensions, which significantly reduces the possibility of using these methods on an industrial scale [6–9].

To overcome this limitation, in recent years, studies of new SPD processes have been conducted in various directions. One of such directions is the development of new
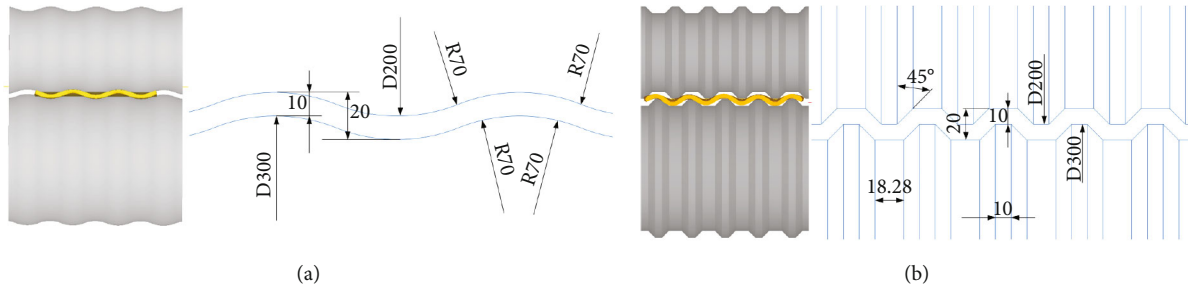
FIGURE 1: Rolling of the workpiece in rolls with (a) radial and (b) trapezoidal relief (all sizes in millimeter).
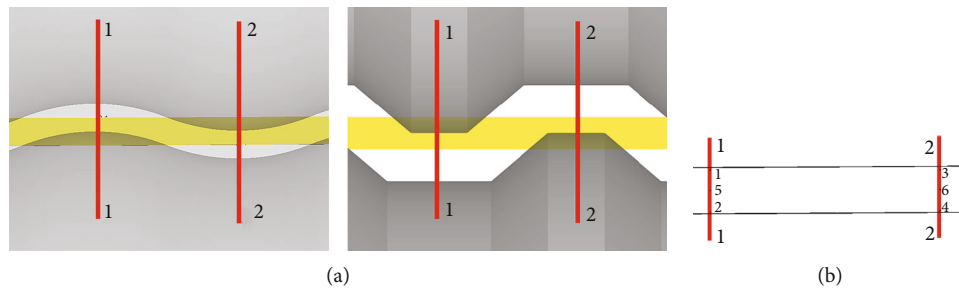

FIGURE 2: Location of points for studying stress-strain state parameters.

deformation schemes of massive workpieces processing during forging [10–12], the key feature of which is an increased level of metal processing due to shear and alternating strains. Another direction of research is the development of new deformation schemes for long-length workpieces. Among the first such technologies are the Conform and Linex processes, modifications of which are being created at the present time [13, 14]. For the possibility of deformation of long-length samples, a number of ECAP-based combined processes have been developed, which also ensure the continuity of the process [15–17].

One of the most known SPD process of rolling type is the accumulative roll bonding process. It is based on the principle when two sheets of the same thickness are rolled with 50% compression by pass [18–20]. The obtained billet is cut for two sheets, which can be rolled again after the surface treatment. As a result, the sheets are joined together, due to the diffusion interaction in the solid phase.

Cross-ARB process (CARB) is a rolling method similar to the ARB process, but with the difference that after each deformation cycle, the rolling direction changes by 90° [21, 22]. This method reduces the plastic anisotropy of sheets and provides a higher level of strength and plastic properties. The main difficulty in implementing ARB and CARB processes is the need for special surface preparation of the sheets to be joined, as well as cutting the side edges, which reduces the manufacturability of these processes.

Asymmetric rolling, which is one of the most promising methods of rolling production, deserves special mention as an SPD process. The use of the asymmetry factor during rolling makes it possible to significantly increase the level of metal processing by pass, as well as to provide the increased level of strength characteristics [23–25]. Asymme-

try during rolling can be created purposefully by mismatch of the circumferential speeds of the rolls when using individual engines, differences in the diameters of the rolls, the use of a roll without a drive (idle roll), and different values of the friction coefficient on the rolls [26–29]. A great contribution to the development of asymmetric rolling was made by the scientific school of A. Pesin; during the research, an industrial installation was created in the form of an asymmetric cold rolling mill. This mill allows rolling steel samples with compression of 75-80% by pass. In the result, an ultrafine-grained structure is obtained. As a result of the conducted studies, it was possible to achieve a gradient between the upper and lower surfaces of the sheet, which can reach 25%. This feature made it possible to obtain both plastic and durable metal, while it was possible to reduce the rolling force by 2-4 times compared to conventional symmetrical rolling [30].

At the same time, the classical theory of asymmetric rolling usually implies the use of smooth rolls. In this case, the main level of processing develops in the longitudinal direction of the workpiece. In [31], a new scheme of asymmetric rolling was proposed, the key feature of which is a relief profile along the entire width of the rolls. The implementation of asymmetric rolling in such rolls leads to simultaneous processing of the metal in the longitudinal and transverse directions. The authors of the work [31] also conducted studies of this rolling method, as a result of which it was found that the most optimal value of the asymmetry coefficient is 1.5.

In [32], the results of simulation the rolling process in relief rolls with various types of asymmetries were presented. As a result, it was revealed that contact asymmetry is the least effective option, and kinematic and geometric
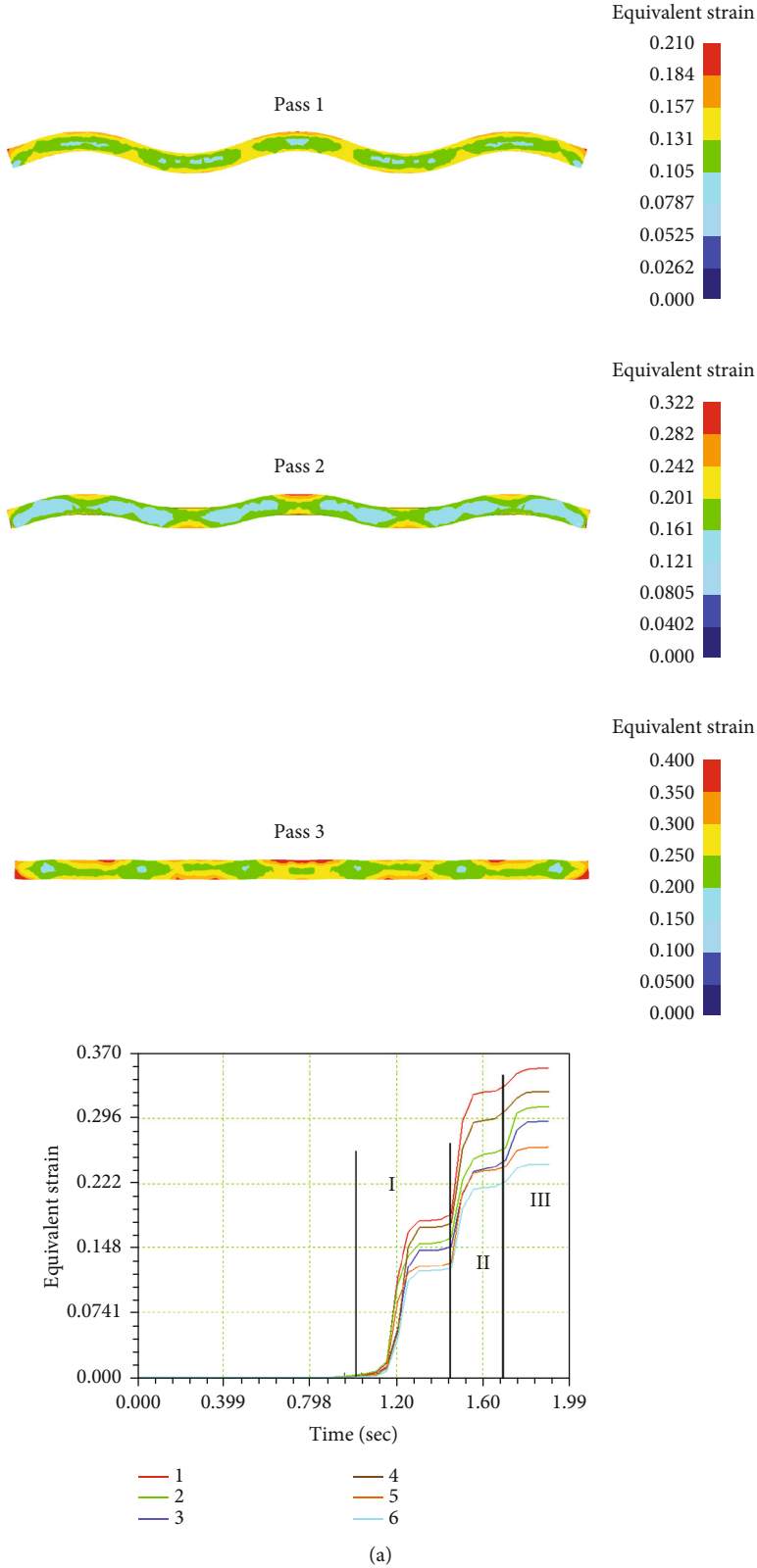
(a)

Figure 3: Continued.

Pass 1

Equivalent strain

| 1.65 |
| 1.44 |
| 1.24 |
| 1.03 |
| 0.825 |
| 0.619 |
| 0.412 |
| 0.206 |
| 0.000 |

Pass 2

Equivalent strain

| 1.52 |
| 1.33 |
| 1.14 |
| 0.950 |
| 0.760 |
| 0.570 |
| 0.380 |
| 0.190 |
| 0.000 |

Pass 3

Equivalent strain

| 1.73 |
| 1.51 |
| 1.30 |
| 1.08 |
| 0.865 |
| 0.649 |
| 0.433 |
| 0.216 |
| 0.000 |

— 1   — 4
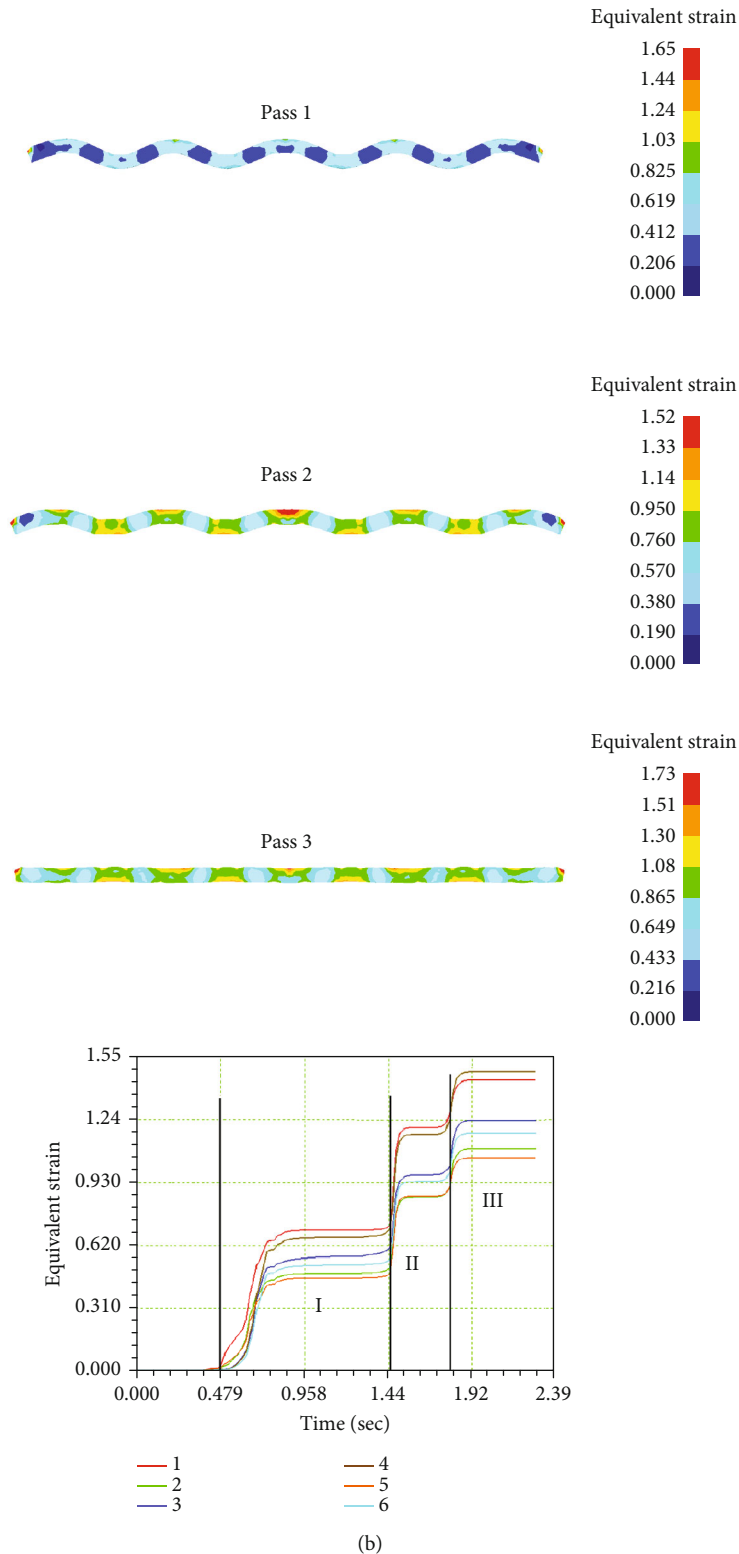— 2   — 5
— 3   — 6

(b)

FIGURE 3: Contour maps and graphs of distribution of equivalent strain during rolling in rolls with (a) radial and (b) trapezoidal relief and leveling in smooth rolls.

asymmetries provide good results in terms of the development of an additional level of shear strain in the longitudinal direction.

The purpose of this work is finite element modeling of asymmetric rolling of a thick-sheet billet of C11000 copper alloy in relief rolls in order to analyze the effectiveness of

possible roll profiles and technological deformation schemes. This type of rolled copper alloys is actively used in the manufacture of heating equipment due to good thermal conductivity. Also, this rolled metal is used in the manufacture of radio equipment and electric generators.

Modeling of deformation processes by the finite element method is one of the most effective methods of theoretical research. In this case, the researcher has the opportunity to look inside the deformation process at any stage, evaluate all the parameters that arise, compare them with critical values, and make necessary adjustments to geometric or technological factors. Another important aspect of using FEM is the assessment of the possibility of stable deformation during the development of a new technological scheme. The scientific innovation of this work lies in determining the patterns of development of stress-strain state parameters for various configurations of rolls, as well as determining the effectiveness of metal processing using various technological schemes. The practical importance of the work lies in the fact that theoretical results obtained in the article will be useful as a basis for creating an industrial installation of this deformation process, or for upgrading an existing rolling mill.

Taking into account the fact that experimental studies of this process are planned to be carried out at a two-stand laboratory rolling mill located at the Karaganda Industrial University, it was decided to consider a variant with geometric asymmetry. This type of asymmetry is the most optimal option due to the fact that the mill bed allows to install rolls of different diameters and develop an asymmetry coefficient up to 1.5 (200 mm and 300 mm). At the same time, the implementation of kinematic asymmetry seems to be an irrational task, since it will require a complete reconstruction of the drive unit of the crate to ensure individual rotation of each roll.

2. Materials and Methods

DEFORM program (SFTC, Columbus, Ohio, USA) was used for the FEM simulation of the investigated deformation technology. The roll diameter with a relief surface was 200 mm for the upper roll and 300 mm for the lower roll. The bevel angle on the protrusions and depressions was 45°. The blank is a rectangular sheet with a cross section of 10×150 mm and a length of 200 mm. C11000 copper alloy was chosen as the workpiece material. The rheological properties of the workpiece material were taken from the internal material database of DEFORM. The following technological parameters were used in computer simulation of the process:

(i) Workpiece material was isotropic and elastic-plastic; the material of rolls was rigid. The elastic-plastic state of the material is described by the following ratios: $\sigma_{xx} = E\bar{\varepsilon}$ at $\bar{\varepsilon} < \bar{\varepsilon}_Y$ and $\sigma_{xx} = \sigma_Y$ at $\bar{\varepsilon} \geq \bar{\varepsilon}_Y$ (here, $\varepsilon_Y = \sigma_Y/E$—strain yield strength at linear loaded state)

(ii) The type of finite elements is tetrahedral; the number of FE nodes is 33072, and the number of FE is

Table 1: Maximum equivalent strain values.

	Pass 1	Pass 2	Pass 3
Radial relief	0.16	0.32	0.35
Trapezoidal relief	0.7	1.18	1.5

157455; the coefficient of FE condensation in complex geometry zones is 3 (i.e., the volume of elements in the areas of contact with roll relief was 3 times less than in the rest of the workpiece)

(iii) Rolling was carried out at an ambient temperature of 20°C

(iv) Heating temperature of the workpiece before rolling was equal to 20°C

(v) The calculation type was nonisothermal; heat exchange coefficient of the workpiece with the tool was 5000 W/(m^2·°C)

(vi) Heat exchange coefficient of the workpiece with the environment was 0.002 W/(m^2·°C)

(vii) When calculating the contact interaction between the workpiece and the rolls, the Siebel friction was set; to create the most stringent conditions of capture, the friction coefficient on the contact of the metal with the rolls was adopted 0.5 (which corresponds to a roughened surface with a high level of roughness in the complete absence of lubrication)

(viii) Rotation speed of the rolls was 60 rad/s

The calculation was carried out by a direct iterative method using a sparse matrix solver for a higher level of convergence at each step. In the calculation, a time increment was used to maintain high accuracy—1 step was equal to 0.001 seconds.

In addition to the considered relief configuration of rolls in the form of trapezoidal projections and depressions, the configuration of rolls with radial grooves proposed in [33] was also studied.

In both configurations, the gap between the rolls ensures that the height of the workpiece is obtained with a double amplitude, i.e., with a workpiece thickness of 10 mm, the amplitude of the protrusions and depressions can reach 20 mm. To assess the effectiveness of the proposed relief profile, it was decided to conduct a comparative analysis of these two roll designs (Figure 1). After rolling in relief rolls, the workpiece was subjected to sequential alignment in smooth rolls with gaps of 15 mm and 10 mm.

To study the parameters of the stress-strain state, it was decided to use the principle of tracking values at various points of the workpiece section. It was decided to conduct the study in two parallel sections: in section 1-1, where the workpiece falls on the protrusion of the large roll, and in section 2-2, where the workpiece falls into the depression of the large roll (Figure 2(a)). This approach will allow to assess the
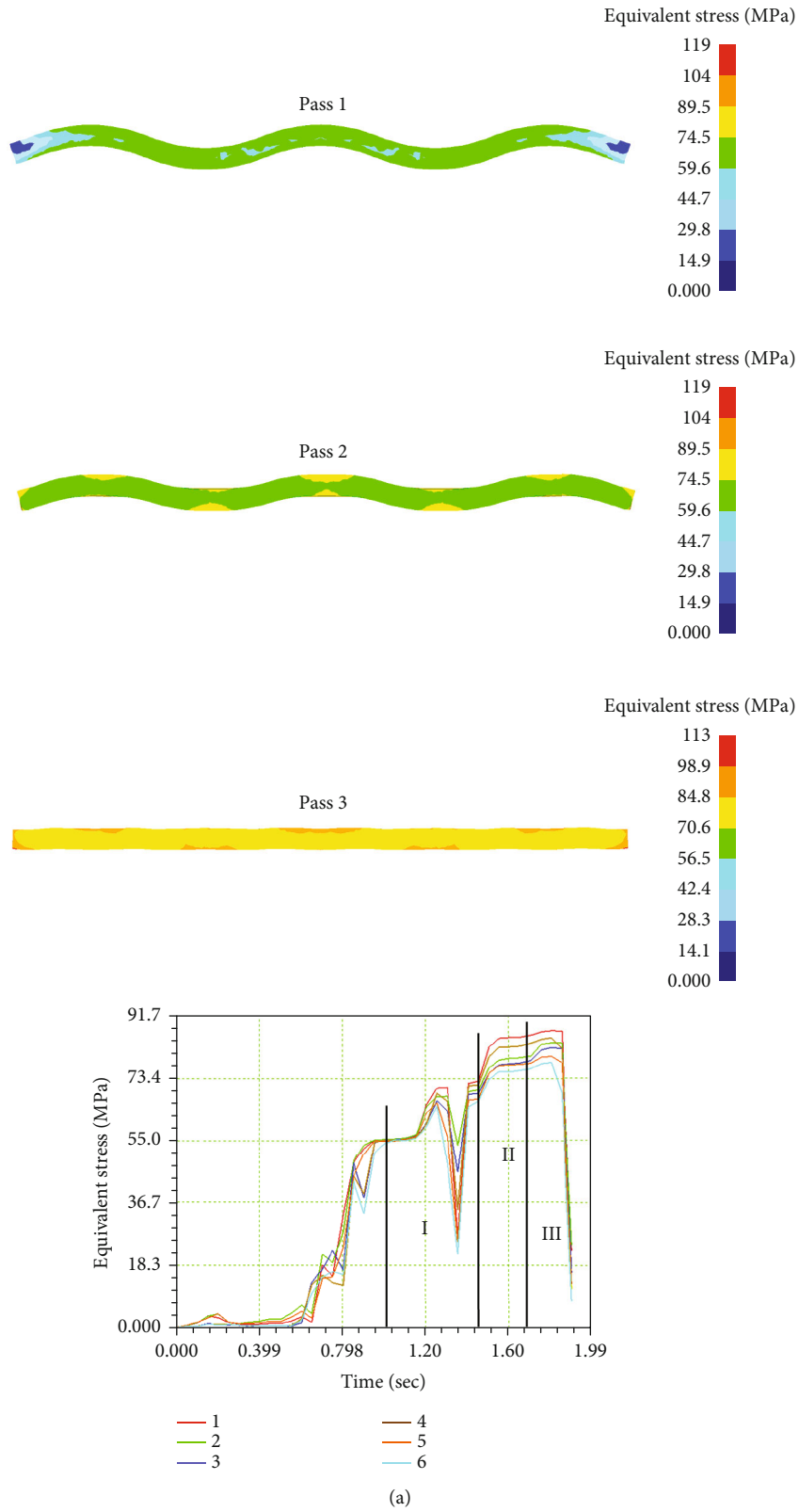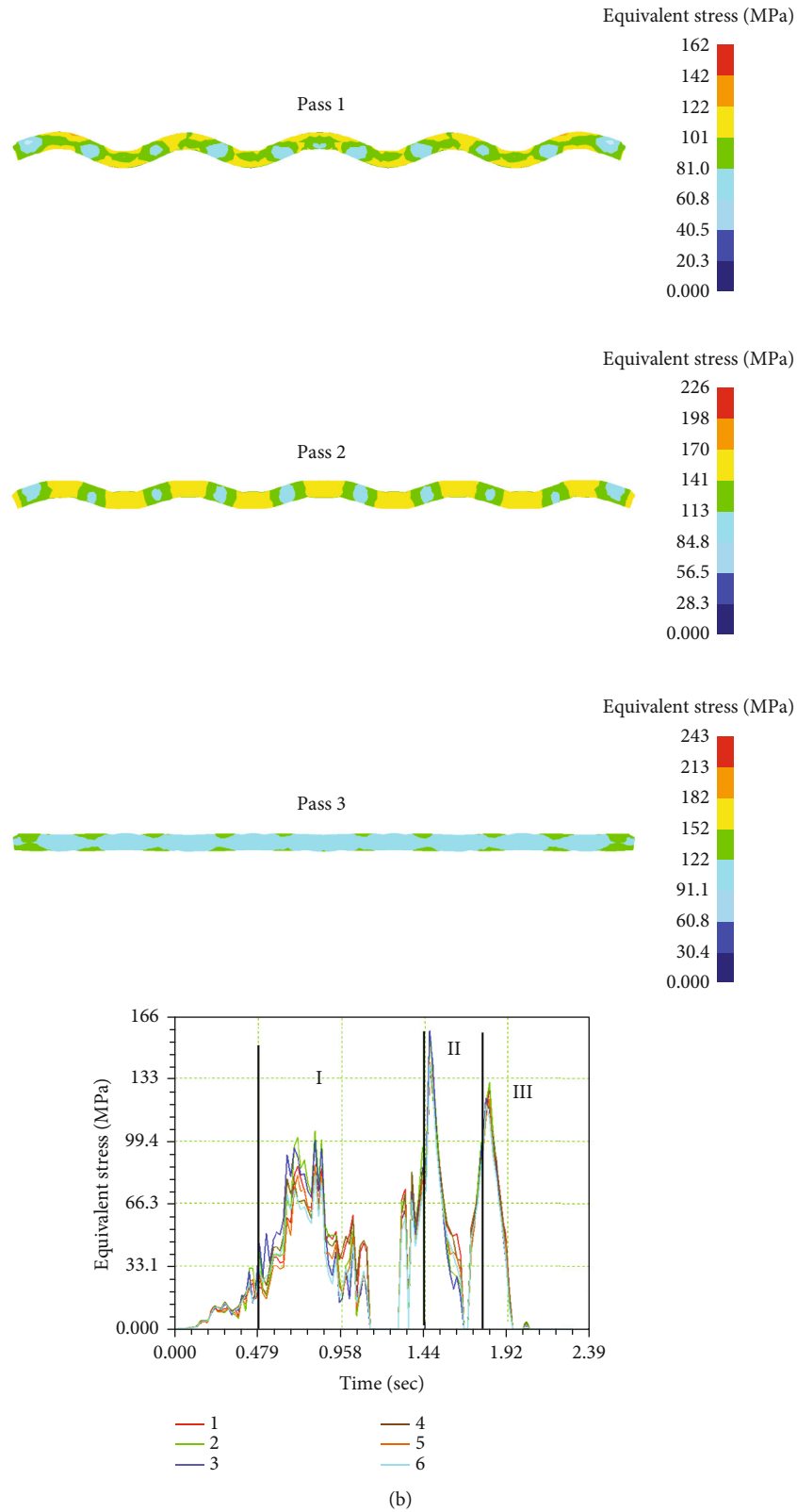
Figure 4: Continued.

FIGURE 4: Contour maps and graphs of distribution of equivalent stress during rolling in rolls with (a) radial and (b) trapezoidal relief and leveling in smooth rolls.

simultaneous influence of the protrusions and depressions of the considered relief of the rolls, taking into account the geometric asymmetry. Three points were made in each section: on the upper and lower surfaces, as well as in the central zone of the workpiece. Figure 2(b) shows the location of 6 points along the section of the workpiece: point 1: on the

surface near the depression of the small roll; point 2: on the surface near the protrusion of the large roll; point 3: on the surface near the protrusion of the small roll; point 4: on the surface near the depression of the large roll; point 5: central area of 1-1 section; and point 6: central area of 2-2 section.

In [32], it was found that one deformation cycle (rolling the workpiece in relief rolls and leveling in smooth rolls to the original shape) is not enough for high-quality metal processing. With multipass deformation, the influence of the number of passes on the processing level is usually investigated. However, this approach for rolling is justified in the case of a symmetrical load from both rolls. In the investigated rolling scheme, it is advisable to consider various technological deformation schemes that will take into account the influence of the asymmetry factor. In the result, the following technological schemes of deformation were proposed:

(1) After the first deformation pass, the workpiece is refed into relief rolls with 180° turning along the axis

(2) After the first deformation pass, the workpiece is refed into relief rolls without any changes of workpiece position

(3) After the first deformation pass, the workpiece is refed into relief rolls with a transverse shift for the relief period. This parameter corresponds to the distance between the previously specified sections 1-1 and 2-2 (Figure 2)

3. Results and Discussion

3.1. Effectiveness of Relief Roll Profiles. When studying the strain state, the equivalent strain (equation (1)) is usually considered for evaluation of the strain intensity. When studying the stress state, the equivalent stress (equation (2)) is usually considered for a general assessment of the stress intensity in the deformation zones and the average hydrostatic pressure (equation (3)) is considered for assessing the level of tensile and compressive stresses.

$$\varepsilon_{\text{EQV}} = \frac{\sqrt{2}}{3} \sqrt{(\varepsilon_1 - \varepsilon_2)^2 + (\varepsilon_2 - \varepsilon_3)^2 + (\varepsilon_3 - \varepsilon_1)^2}, \quad (1)$$

$$\sigma_{\text{EQV}} = \frac{1}{\sqrt{2}} \sqrt{(\sigma_1 - \sigma_2)^2 + (\sigma_2 - \sigma_3)^2 + (\sigma_3 - \sigma_1)^2}, \quad (2)$$

$$\sigma_{\text{AV}} = \frac{\sigma_1 + \sigma_2 + \sigma_3}{3}, \quad (3)$$

where ε_1, ε_2, and ε_3 are the main strains and σ_1, σ_2, and σ_3 are the main stresses.

Considering the key parameter of the strain state "equivalent strain" in both models (Figure 3), it can be noted the similar nature of the distribution. In both cases, the equivalent strain graphs have three successive stages, each of which corresponds to deformation in the deformation zone of the rolling rolls: zone I: rolling in the first pair of relief rolls; zone II: rolling in the second pair of smooth rolls; and zone III:
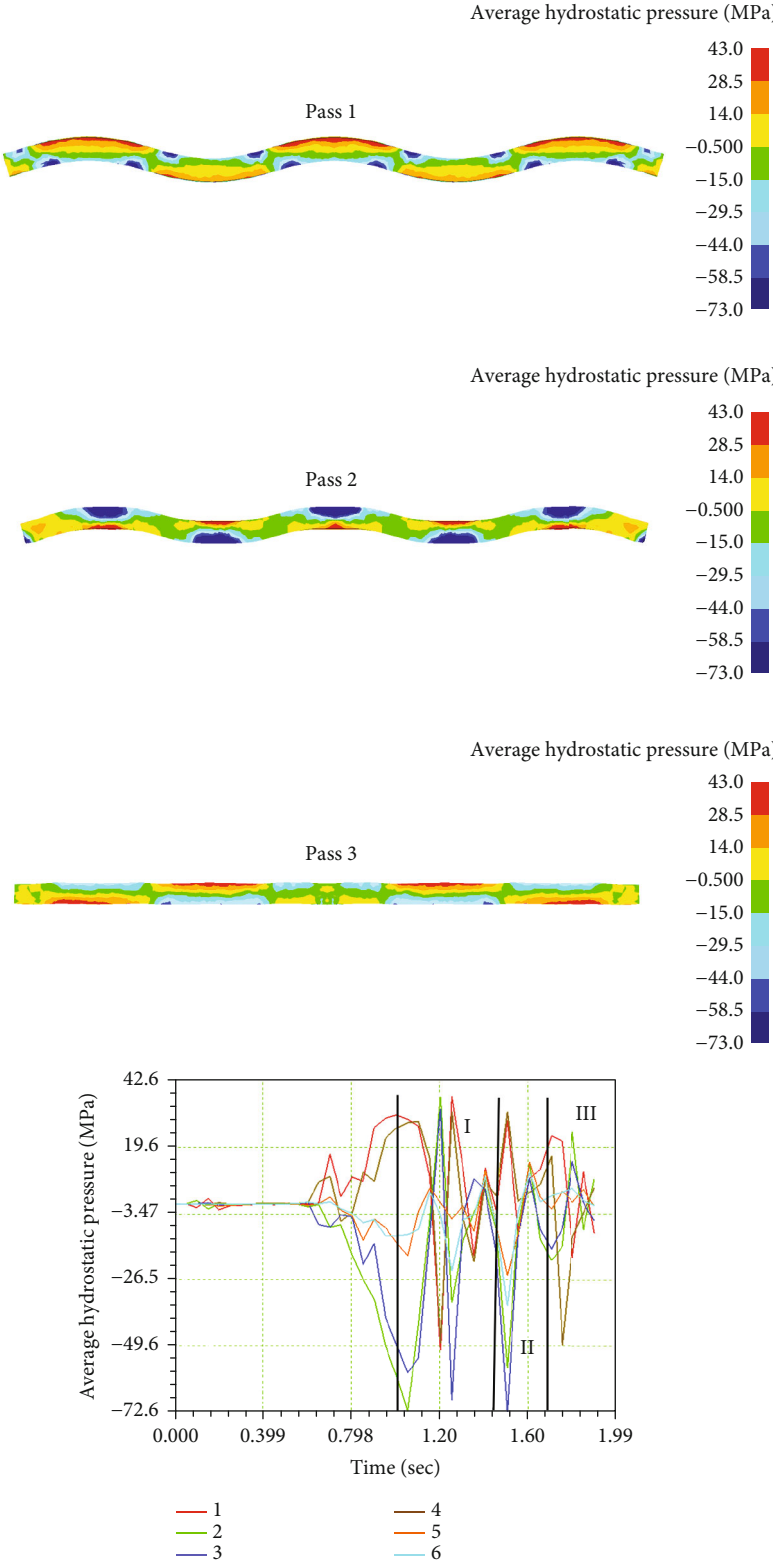
Table 2: Equivalent stress values (MPa).

	Pass 1	Pass 2	Pass 3
Radial relief	70	85	90
Trapezoidal relief	100	160	125

rolling in the third pair of smooth rolls. Taking into account the fact that this parameter is cumulative, it is convenient to track the extent of geometric deformation zones along the boundaries of the accumulation of equivalent strain (vertical black lines).

At the same time, it was found that the use of trapezoidal relief rolls can significantly increase the level of metal processing, which usually implies an increase in the level of equivalent strain. In the radial relief model, the level of equivalent strain increases sequentially to 0.12-0.16 after rolling in the first pair of relief rolls, then to 0.2-0.32 after rolling in the second pair of smooth rolls, and to 0.24-0.35 after rolling in the third pair of smooth rolls (Figure 3(a)). In the trapezoidal relief model, the level of equivalent strain increases sequentially to 0.45-0.7 after rolling in the first pair of relief rolls, then to 0.85-1.18 after rolling in the second pair of smooth rolls, and to 1.05-1.5 after rolling in the third pair of smooth rolls (Figure 3(b)). For ease of comparison, maximum equivalent strain values have been summarized in Table 1.
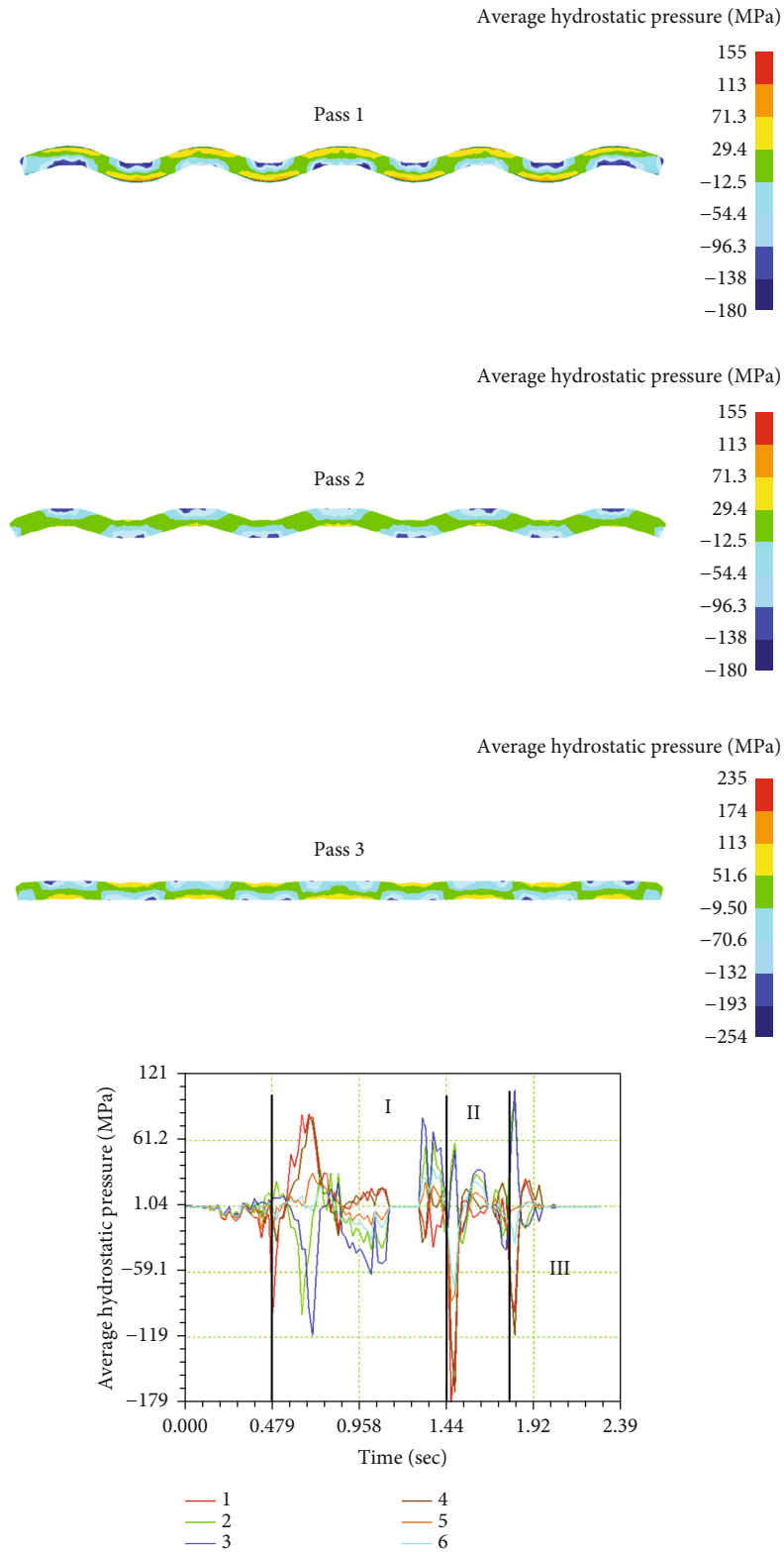
Such a significant difference in the processing level is explained by the fact that the trapezoidal relief of the rolls leads to a more significant shape change of the workpiece during deformation. The presence of ribs on the protrusions inevitably leads to a slight compression of the workpiece, which indicates more stringent conditions for metal capture by rolls.

Analyzing the graphs of equivalent stresses, it can be noted their significant difference in appearance. If the graphs of the model with radial relief have a nonstandard appearance, where the deformation zones are practically not separated from each other (Figure 4(a)), then the graphs of the model with trapezoidal relief have a traditional appearance, where three zones of deformation zones are clearly visible (Figure 4(b)). This effect in the model with radial relief is the result of the fact that the workpiece after leaving the relief rolls has a fairly smooth cross-section shape, which is easily captured by subsequent smooth rolls, as a result of which there is a slight decrease in the stress level before entering zone II. When using a trapezoidal relief, the workpiece has a sharper cross-section shape; at the moment of contact of the workpiece with smooth rolls, its short-term braking and crumpling of the front edges occur. As a result, the stress is reduced to zero. After increasing the contact area, the metal is captured by the rolls, which leads to a stress jump. Comparing the stress level, it was revealed that the use of radial relief causes an increase in stresses up to 90 MPa, whereas when using trapezoidal relief, the stress level reaches 100 MPa in relief rolls and 160 MPa when the relief billet hits smooth rolls. For ease of comparison, all equivalent stress values have been summarized in Table 2.

Average hydrostatic pressure (MPa)

Pass 1

	43.0
	28.5
	14.0
	−0.500
	−15.0
	−29.5
	−44.0
	−58.5
	−73.0

Average hydrostatic pressure (MPa)

Pass 2

	43.0
	28.5
	14.0
	−0.500
	−15.0
	−29.5
	−44.0
	−58.5
	−73.0

Average hydrostatic pressure (MPa)

Pass 3

	43.0
	28.5
	14.0
	−0.500
	−15.0
	−29.5
	−44.0
	−58.5
	−73.0

(a)

Figure 5: Continued.

Average hydrostatic pressure (MPa)

Pass 1

155	
113	
71.3	
29.4	
−12.5	
−54.4	
−96.3	
−138	
−180	

Average hydrostatic pressure (MPa)

Pass 2

155	
113	
71.3	
29.4	
−12.5	
−54.4	
−96.3	
−138	
−180	

Average hydrostatic pressure (MPa)

Pass 3

235	
174	
113	
51.6	
−9.50	
−70.6	
−132	
−193	
−254	

(b)

Figure 5: Contour maps and graphs of distribution of average hydrostatic pressure during rolling in rolls with (a) radial and (b) trapezoidal relief and leveling in smooth rolls.

TABLE 3: Average hydrostatic pressure values (MPa).

	Pass 1	Pass 2	Pass 3
Radial relief	-73	-70	-50
Trapezoidal relief	-120	-180	-120

It can be seen from the data in Table 2 that the greatest difference in values (almost 2 times) occurs when rolling in smooth rolls at pass 2. This is the result of the initial alignment of the relief profile, and the radial relief is smoother and easier to align. The trapezoidal relief has clearer shapes, and its alignment requires more energy consumption.

Considering the distribution of the average hydrostatic pressure in both models, it can be noted a similar distribution of stresses in the deformation zone of relief rolls. Here, points 1 and 4 in contact with the relief protrusion experience compressive stresses, while tensile stresses occur on opposite sides at points 2 and 3 (Figure 5). At the same time, in the model with trapezoidal relief, the overall stress level is significantly higher due to more stringent conditions for capturing metal by rolls.

The level of compressive stresses is -65 to -73 MPa approximately when using radial relief and -110 to -120 MPa when using trapezoidal relief. When the second pair of smooth rolls is captured in the model with radial relief, due to the smoother shape of the workpiece, the compressive stress level is -70 MPa approximately, whereas in the model with trapezoidal relief, the compressive stress level reaches -180 MPa. Such a significant increase in compressive stresses is the result of a sharper shape of the workpiece after leaving the relief rolls. When gripping the third pair of smooth rolls, the workpiece is already half aligned, so in both models, the level of compressive stresses is lower here than in the previous stand. At the same time, in the model with trapezoidal relief, a higher stress level is maintained, reaching -120 MPa versus -50 MPa in the model with radial relief. For ease of comparison, average hydrostatic pressure values have been summarized in Table 3.

For EN 1.2550 steel, which was used for the rolls production, the yield strength at 20°C is 1290 MPa. Therefore, it can be concluded that at all three stages of deformation, when using any of the considered configurations, the obtained values of equivalent stress and average hydrostatic pressure do not exceed critical value equal to the yield strength of the roll material. However, for a complete conclusion about the optimal choice of the roll configuration, it is necessary to consider the resulting rolling forces, since this parameter has a significant impact on many components of the rolling mill, such as an electric motor and gearbox.

Comparing the graphs of forces (Figure 6), a higher level in the model with a trapezoidal relief was noted. When rolling in a relief rolls, there is a slight difference in the force level on the rolls. In the trapezoidal relief model, the force on the smaller roll is 205 kN and on the larger roll is 225 kN. In the model with radial relief, the force on the smaller roll is 150 kN and on the larger roll is 165 kN. When the workpiece is captured by the second pair of smooth rolls

in the model with radial relief, the force is 57 kN, whereas in the model with trapezoidal relief, the force is 205 kN. This significant difference correlates well with the difference in emerging stresses due to more stringent capture conditions. Comparing the efforts of the second and third pairs of smooth rolls, it was noted that in both models, the force level in the third pass is higher than in the second pass. This is due to the fact that the workpiece after the second pass has a cross-section shape close to the initial one. This leads to an increase in the contact surface area when the metal is captured by the third pair of rolls. When the workpiece is captured by the third pair of smooth rolls in the model with radial relief, the force is 100 kN, whereas in the model with trapezoidal relief, the force is 265 kN.

For ease of comparison, all force values have been summarized in Table 4. Here, for pass 1 in relief rolls, the numerator indicates the forces for the small roll and the denominator for the large roll. It can be seen from the data in Table 4 that the greatest difference in values occurs when rolling in smooth rolls. This is the result of the fact that after the first pass, the workpieces have cross-section profiles that differ greatly from each other. However, the radial profile has a smoother shape and therefore requires less energy to align.

These force indicators demonstrate results that are opposite to the comparison of equivalent strain. When analyzing the strain state, it was found that the trapezoidal roll profile would be the optimal choice due to a higher level of equivalent strain. In this case the radial roll profile would be the best option, since it would require significantly less energy consumption. The final choice of the roll configuration must be made based on the force values obtained and the known strength level of the rolling equipment. If it is possible to use a trapezoidal configuration without potential equipment failure, this type of relief will be the preferred choice; otherwise, at low values of equipment strength, a radial roll configuration should be used.

As a result of comparing the main parameters of the stress-strain state and the deformation force in the considered models with different types of relief rolls, the following conclusions can be drawn:

(1) The use of trapezoidal relief allows to increase the level of metal processing by almost 5 times compared with the use of radial relief

(2) The level of compressive stresses when using trapezoidal relief is 1.5 times higher than using radial relief. With subsequent capture by smooth rolls, the level of compressive stresses in the model with trapezoidal relief is 2.5 times higher, which is the optimal condition for closing possible internal defects. In both cases, the obtained values of equivalent stress and average hydrostatic pressure do not exceed critical value equal to the yield strength of the roll material

(3) The force level in the model with trapezoidal relief in the first pass is 1.4 times higher and in smooth passages is 2.6 and 3.6 times higher, respectively
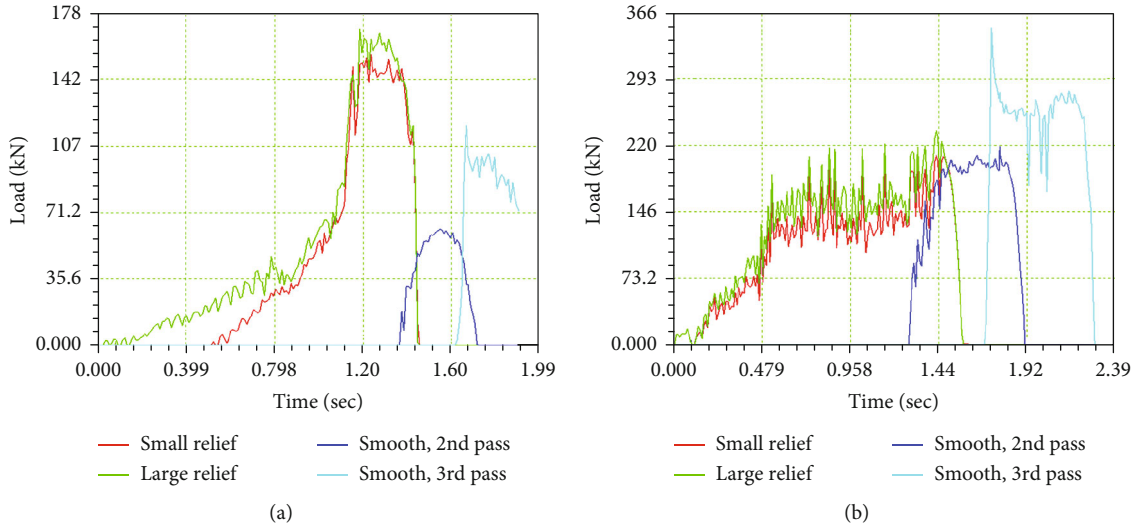
(a)

(b)

Figure 6: Rolling force in rolls with (a) radial and (b) trapezoidal relief and leveling in smooth rolls.

Table 4: Roll forces (kN).

	Pass 1	Pass 2	Pass 3
Radial relief	150/165	57	100
Trapezoidal relief	205/225	205	265

Taking into account the obtained differences in values, the most effective solution for the implementation of rolling in relief rolls will be the use of trapezoidal relief. At the same time, it is necessary to take into account the obtained force level and use the trapezoidal relief only in case of sufficient strength of the rolling equipment.

3.2. Effectiveness of Technological Schemes of Deformation. To assess the effectiveness of technological deformation schemes, equivalent strain was considered as a key parameter of the metal processing. Figures 7–9 show graphs of equivalent strain after two passes for the three technological deformation schemes. Here, points 1 and 3 correspond to the surface zones, and point 2 corresponds to the axial region. When the workpiece is turned by 180°, there is a sequential contact of both horizontal faces with each roll. As a result, the influence of the asymmetry factor is minimal, since each face alternately has contact with a roll of a larger diameter. This is clearly seen when considering the values of the equivalent strain on each pass. After the first pass (stage 3) and after the second pass (stage 6), the strain difference between the surface zones decreases to 0.15. At the same time, the maximum strain level is 2.4, and the minimum is 1.93 (Figure 7).

When deforming without changing the workpiece position, double identical contact of the workpiece and the rolls occurs. As a result, the influence of the asymmetry factor is maximal, since each face has contact with only one roll and only with a certain relief zone. This leads to the fact that the difference in the values of the equivalent strain after the
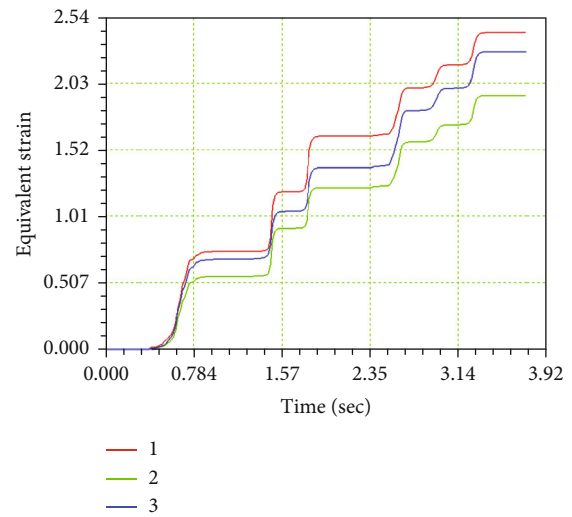

Figure 7: Equivalent strain after two passes with 180° workpiece turning between passes.

first pass (stage 3) increases significantly to 0.6 after the second pass (stage 6). At the same time, the maximum strain level is 3.5, and the minimum is 2.6 (Figure 8).

When deforming with a workpiece shift for the relief period, there is a double contact of the workpiece and the rolls, but here, each face has contact with different relief zones. As a result, the influence of the asymmetry factor is quite high, but there is no increase in the difference of equivalent strain, which remains at the level of 0.4. At the same time, the maximum strain level is 2.8, and the minimum is 2.3 (Figure 9).

Comparison of technological schemes of deformation showed that the choice of scheme will depend on the desired result, i.e., on the required level of uniformity of properties across the section. At the same time, it is necessary to note certain features of the practical implementation of each
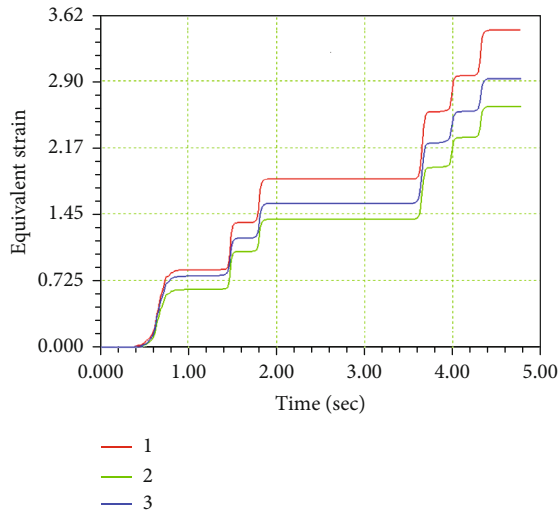
FIGURE 8: Equivalent strain after two passes without changing the workpiece position.
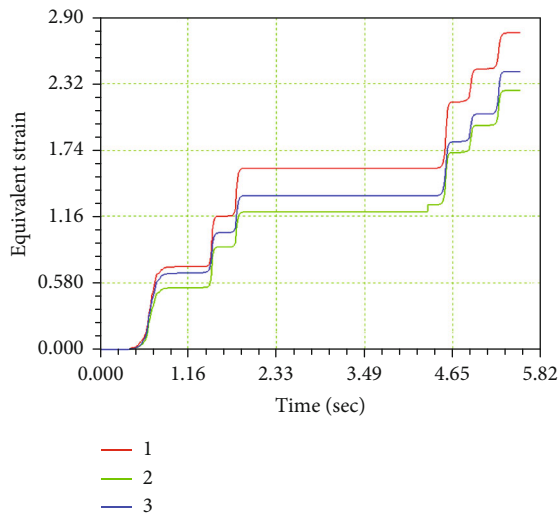

FIGURE 9: Equivalent strain after two passes with transverse shift of the workpiece for the relief period.

scheme. Deformation with 180° workpiece turning between passes significantly reduces the influence of the asymmetry factor. This is reflected in the level of equivalent strain and its difference in the workpiece height. The choice of this deformation scheme for practical implementation will be associated with the additional operation of turning the workpiece 180° along the rolling axis, which will require auxiliary equipment.

Deformation without changing the workpiece position between the passes has the opposite effect, and such a scheme significantly increases the influence of the asymmetry factor. The implementation of this scheme is the simplest, since it does not require any additional operations or equipment.

Deformation with a transverse workpiece shift for the relief period between passes has the effect of a "golden
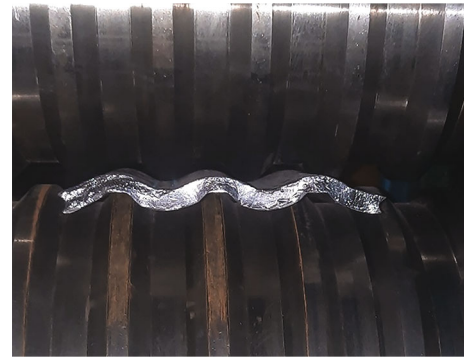

FIGURE 10: Rolling of the workpiece in relief rolls.

mean" when the influence of asymmetry takes place, but the difference in strain values is not as large as in the previous case. The implementation of this scheme will require visual or automatic control of the shift magnitude for the relief period by reconfiguring the guide lines.

3.3. Experimental Deformation of Lead and Copper Workpieces. In order to test the developed technology, as well as to verify the data on the shape change obtained by computer simulation, a laboratory experiment on a lead blank was conducted. For correct comparison of the results of the experiment with modeling, an additional model of asymmetric rolling in relief rolls for lead billet with identical geometric parameters was calculated, where only the study of shape change was carried out. The geometric parameters of the workpiece and rolls were completely identical during simulation and experiment, and a blank with a thickness of 10 mm and a width of 150 mm was selected. The roll rotation speed and the gaps between the smooth rolls also corresponded to the values adopted when modeling the copper billet. The laboratory experiment was carried out in accordance with the developed deformation technology—after rolling in relief rolls (Figure 10), the workpiece was leveled in smooth rolls. A corresponding finite element model was constructed for the same conditions.

At the same time, the gap at the second stage of leveling (3rd pass) was equal to the thickness of the workpiece, and at the first stage of leveling, the gap was set as half the difference in the workpiece height before and after rolling in relief rolls. It was previously revealed that the height of the workpiece after the first pass increases by 75-80% [34]. According to this principle, the gap in the second passage was equal to 14 mm. After rolling in relief rolls and the subsequent two stages of leveling, the workpiece had the form shown in Figure 11. For comparison, the height and width of the workpiece during simulation are shown on the left. Taking into account the fact that the material in finite element modeling is completely homogeneous, when considering the width in the perpendicular direction of view, it is very difficult to see protrusions and depressions. Therefore, for clarity, the width of the model blank is shown in the isometry.
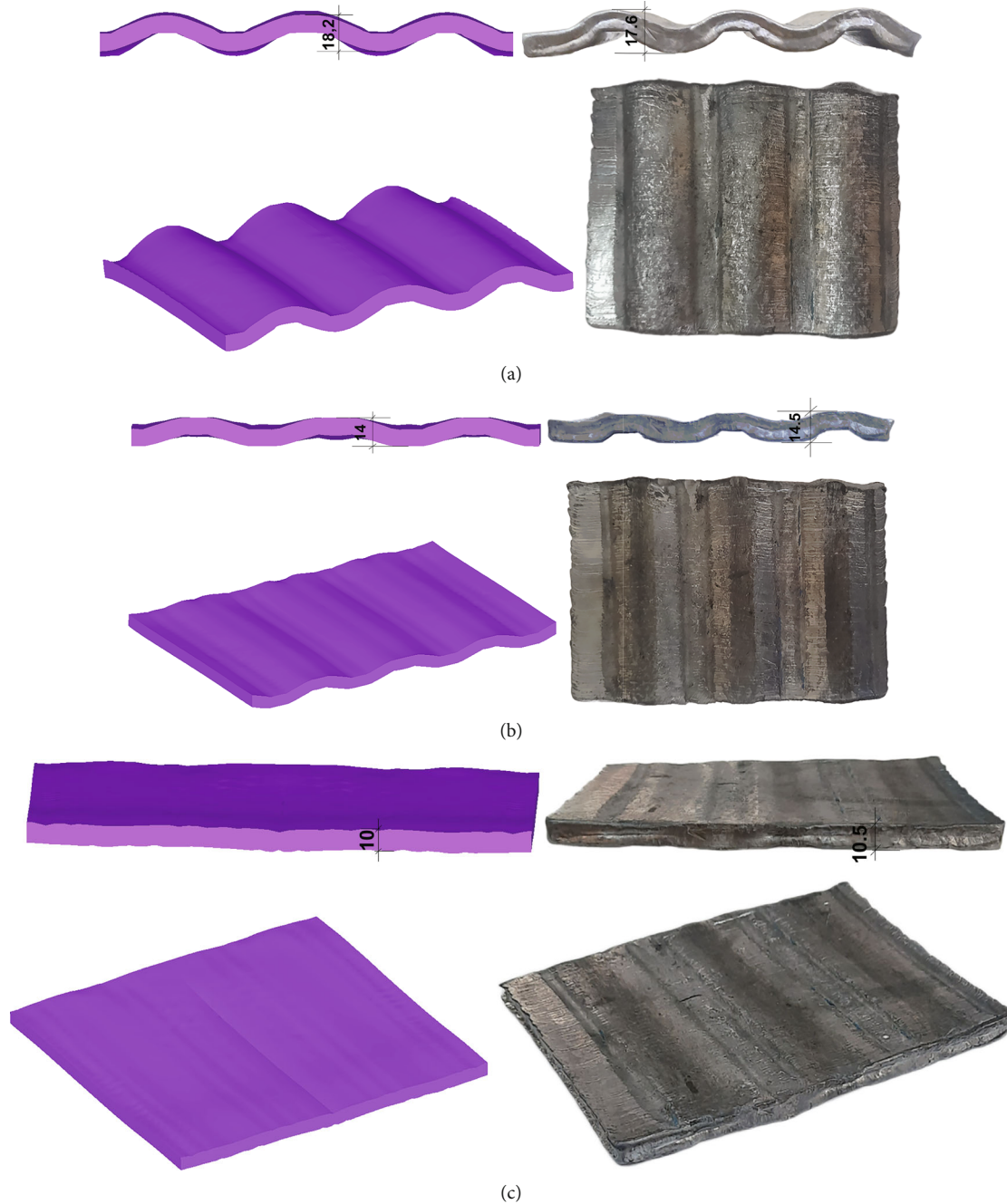
FIGURE 11: Comparison of the shape of a lead billet in modeling and experiment: (a) after rolling in relief rolls; (b) after the 1st stage of alignment; (c) after the 2nd stage of alignment.

TABLE 5: Height amplitude values of lead workpiece.

	Pass 1 (mm)	Difference (%)	Pass 2 (mm)	Difference (%)	Pass 3 (mm)	Difference (%)
Simulation	18.2		14		10	
		3.29		3.57		5
Experiment	17.6		14.5		10.5	

Table 5 shows the height amplitude values for each pass. The differences of the obtained values in percentages are also shown.

A comparison of the geometric parameters of the workpiece after rolling in relief rolls and two subsequent alignment passes in smooth rolls showed that the results of
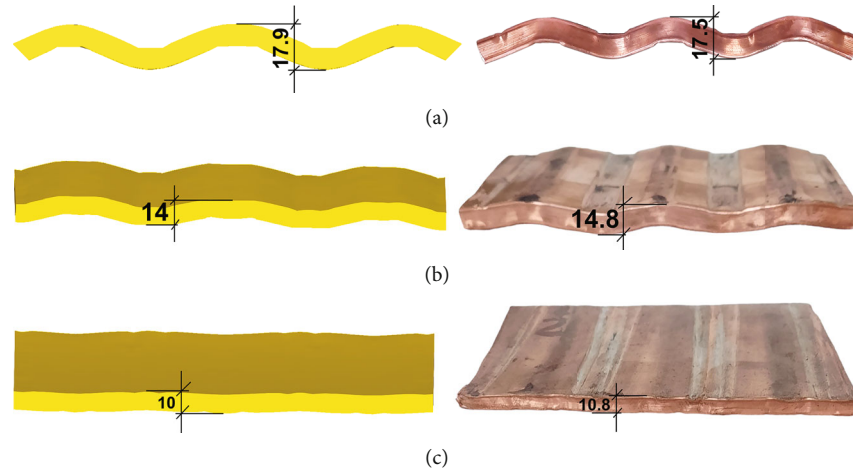
FIGURE 12: Comparison of the shape of a copper billet in modeling and experiment: (a) after rolling in relief rolls; (b) after the 1st stage of alignment; (c) after the 2nd stage of alignment.

TABLE 6: Height amplitude values of copper workpiece.

	Pass 1 (mm)	Difference (%)	Pass 2 (mm)	Difference (%)	Pass 3 (mm)	Difference (%)
Simulation	17.9		14		10	
		2.28		5.7		8
Experiment	17.5		14.8		10.8	

computer simulation have a high level of convergence. At each deformation stage, the difference in the geometric parameters of the workpiece between the model and the experiment did not exceed 3-5%.

After preliminary asymmetric rolling of the lead billet in relief rolls, a similar experiment to deform a workpiece of M1 copper alloy with a thickness of 10 mm and a width of 150 mm was conducted. Figure 12 shows the comparison results of the workpiece shape during modeling and experiment at all deformation stages.

Table 6 shows the height amplitude values for each pass. The increased difference values at the alignment stages are the result of the fact that the rolling cage of a laboratory mill with smooth rolls has smaller dimensions and, as a result, less structural rigidity. Therefore, when rolling a harder material, there is an increase in the gap between the rolls. In real conditions, all rolling cages have a higher level of rigidity, as well as special mechanisms to create an antibending effect of the rolls.

4. Conclusion

Conducted finite element simulation of asymmetric rolling in relief rolls of C11000 copper alloy in order to analyze the effectiveness of possible roll profiles and technological schemes of deformation was revealed that despite the increased level of stress and force, the use of trapezoidal relief makes it possible to increase the level of metal processing by almost 5 times compared with the use of radial relief. Deformation with 180° workpiece turning between passes significantly reduces the influence of the asymmetry factor.

The choice of this deformation scheme for practical implementation will require auxiliary equipment for turning operation. Deformation without changing the workpiece position between the passes significantly increases the influence of the asymmetry factor and does not require any additional operations or equipment. Deformation with a transverse workpiece shift for the relief period between passes has average level of asymmetry influence, and it will require visual or automatic control of the shift magnitude for the relief period by reconfiguring the guide lines. A preliminary laboratory experiment of lead rolling revealed a high convergence level with results of computer simulation. At each deformation stage, the difference in the geometric parameters of the workpiece between the model and the experiment did not exceed 3-5%. When deforming a copper billet, the maximum difference level was 8%, which is the result of the low rigidity of the rolling cage with smooth rolls. The theoretical results obtained in the article will be useful as a basis for creating an industrial installation of this deformation process, or for upgrading an existing rolling mill.

Data Availability

The DEFORM databases used in this study are available from the corresponding author upon request.

Conflicts of Interest

The authors declare that there are no conflicts of interest regarding the publication of this paper.

References

[1] R. Z. Valiev, R. K. Islamgaliev, and I. V. Alexandrov, "Bulk nanostructured materials from severe plastic deformation," *Progress in Materials Science*, vol. 45, no. 2, pp. 103–189, 2000.

[2] R. Z. Valiev and T. G. Langdon, "Principles of equal-channel angular pressing as a processing tool for grain refinement," *Progress in Materials Science*, vol. 51, no. 7, pp. 881–981, 2006.

[3] T. Sakai, A. Belyakov, R. Kaibyshev, H. Miura, and J. J. Jonas, "Dynamic and post-dynamic recrystallization under hot, cold and severe plastic deformation conditions," *Progress in Materials Science*, vol. 60, no. 1, pp. 130–207, 2014.

[4] N. Tsuji, Y. Ito, Y. Saito, and Y. Minamino, "Strength and ductility of ultrafine grained aluminum and iron produced by ARB and annealing," *Scripta Materialia*, vol. 47, no. 12, pp. 893–899, 2002.

[5] R. Z. Valiev, I. V. Alexandrov, Y. T. Zhu, and T. C. Lowe, "Paradox of strength and ductility in metals processed by severe plastic deformation," *Journal of Materials Research*, vol. 17, no. 1, pp. 5–8, 2002.

[6] A. P. Zhilyaev and T. G. Langdon, "Using high-pressure torsion for metal processing: fundamentals and applications," *Progress in Materials Science*, vol. 53, no. 6, pp. 893–979, 2008.

[7] M. Emerla, P. Bazarnik, Y. Huang, M. Lewandowska, and T. G. Langdon, "Using direct high-pressure torsion synthesis to produce aluminium matrix nanocomposites reinforced with carbon nanotubes," *Journal of Alloys and Compounds*, vol. 968, article 171928, 2023.

[8] J. A. Muñoz, M. Chand, J. W. Signorelli, J. Calvo, and J. M. Cabrera, "Strengthening of duplex stainless steel processed by equal channel angular pressing (ECAP)," *International Journal of Advanced Manufacturing Technology*, vol. 123, no. 7-8, pp. 2261–2278, 2022.

[9] M. Zohrevand, M. Mohammadi-Zerankeshi, F. Nobakht-Farin, R. Alizadeh, and R. Mahmudi, "Degradation behavior of the as-extruded and ECAP-processed Mg-4Zn alloy by Ca addition and hydrothermal coating," *Journal of Materials Research and Technology*, vol. 20, pp. 1204–1215, 2022.

[10] V. Kukhar, E. Balalayeva, S. Hurkovska et al., "The selection of options for closed-die forging of complex parts using computer simulation by the criteria of material savings and minimum forging force," *Advances in Intelligent Systems and Computing*, vol. 989, pp. 325–331, 2020.

[11] V. V. Drahobetsky, A. A. Shapoval, V. T. Shchetynin et al., "New solution for plastic deformation process intensification," *Metallurgist*, vol. 65, no. 9-10, pp. 1108–1116, 2022.

[12] O. E. Markov, A. S. Khvashchynskyi, A. V. Musorin, M. A. Markova, A. A. Shapoval, and N. S. Hrudkina, "Investigation of new method of large ingots forging based on upsetting of workpieces with ledges," *International Journal of Advanced Manufacturing Technology*, vol. 122, no. 3-4, pp. 1383–1394, 2022.

[13] N. H. Ghaforian, M. Gerdooei, K. Khalili, and M. Mohammadi, "Usability of the ECAP-conform process for the production of dental implants material," *Journal of the Mechanical Behavior of Biomedical Materials*, vol. 147, article 106124, 2023.

[14] E. Panin, I. Volokitina, A. Volokitin et al., "Finite element modeling of ECAP-Linex combined process of severe plastic deformation," *Modelling and Simulation in Engineering*, vol. 2023, Article ID 1573884, 23 pages, 2023.

[15] M. V. Chukin, A. G. Korchunov, M. A. Polyakova, and D. G. Emaleeva, "Forming ultrafine-grain structure in steel wire by continuous deformation," *Steel in Translation*, vol. 40, no. 6, pp. 595–597, 2010.

[16] D. V. Konstantinov, A. G. Korchunov, M. V. Zaitseva, O. P. Shiryaev, and D. G. Emaleeva, "Macro- and micromechanics of pearlitic-steel deformation in multistage wire production," *Steel in Translation*, vol. 48, no. 7, pp. 458–462, 2018.

[17] A. Naizabekov, S. Lezhnev, E. Panin et al., "Effect of combined rolling–ECAP on ultrafine-grained structure and properties in 6063 Al alloy," *Journal of Materials Engineering and Performance*, vol. 28, no. 1, pp. 200–210, 2019.

[18] D. Rahmatabadi, M. Tayyebi, R. Hashemi, and G. Faraji, "Evaluation of microstructure and mechanical properties of multi-layer Al5052-Cu composite produced by accmulative roll bonding," *Powder Metallurgy and Metal Ceramics*, vol. 57, no. 3-4, pp. 144–153, 2018.

[19] M. Tayyebi, D. Rahmatabadi, A. Karimi, M. Adhami, and R. Hashemi, "Investigation of annealing treatment on the interfacial and mechanical properties of Al5052/Cu multilayered composites subjected to ARB process," *Journal of Alloys and Compounds*, vol. 871, article 159513, 2021.

[20] D. Rahmatabadi, A. Shahmirzaloo, R. Hashemi, and M. Farahani, "Using digital image correlation for characterizing the elastic and plastic parameters of ultrafine-grained Al 1050 strips fabricated via accumulative roll bonding process," *Materials Research Express*, vol. 6, no. 8, article 086542, 2019.

[21] N. Kalantarrashidi, M. Alizadeh, and S. Pashangeh, "Consideration on zinc content on the microstructure, mechanical, and corrosion evolution of aluminum/zinc composites fabricated by CARB process," *Journal of Materials Research and Technology*, vol. 19, pp. 1805–1820, 2022.

[22] M. Naseri, M. Reihanian, A. O. Moghaddam et al., "Insights into the mechanical properties and correlation between strain path and crystallographic texture of the AA2024 alloy during severe plastic deformation," *Metals and Materials International*, vol. 30, no. 2, pp. 412–424, 2024.

[23] A. M. Pesin, V. M. Salganik, D. O. Pustovoitov, and H. Dyja, "Asymmetric rolling: theory and technology," *Hutnik-Wiadomości Hutnicze*, vol. 5, pp. 358–363, 2012.

[24] G. Vincze, F. Simões, and M. Butuc, "Asymmetrical rolling of aluminum alloys and steels: a review," *Metals*, vol. 10, p. 1126, 2020.

[25] D. Pustovoytov, A. Pesin, and P. Tandon, "Asymmetric (hot, warm, cold, cryo) rolling of light alloys: a review," *Metals*, vol. 11, p. 956, 2021.

[26] Y. H. Ji and J. J. Park, "Development of severe plastic deformation by various asymmetric rolling processes," *Materials Science and Engineering A*, vol. 499, no. 1-2, pp. 14–17, 2009.

[27] L. L. Chang, J. H. Cho, and S. B. Kang, "Microstructure and mechanical properties of AM31 magnesium alloys processed by differential speed rolling," *Journal of Materials Processing Technology*, vol. 211, no. 9, pp. 1527–1533, 2011.

[28] W. J. Kim, Y. G. Lee, M. J. Lee, J. Y. Wang, and Y. B. Park, "Exceptionally high strength in Mg-3Al-1Zn alloy processed

by high-ratio differential speed rolling," *Scripta Materialia*, vol. 65, no. 12, pp. 1105–1108, 2011.

[29] H. Gao, S. C. Ramalingam, G. C. Barber, and G. Chen, "Analysis of asymmetrical cold rolling with varying coefficients of friction," *Journal of Materials Processing Technology*, vol. 124, no. 1-2, pp. 178–182, 2002.

[30] N. V. Koptseva, Y. Y. Efimova, A. M. Pesin, and M. V. Chukin, "Investigation of the features of the formation of the structure of steel 08Yu during asymmetric rolling on a new mill 400," *Chernye Metally*, vol. 2022, no. 10, pp. 39–44, 2022.

[31] A. B. Naizabekov, S. N. Lezhnev, E. A. Panin, A. A. Tymchenko, and A. B. Esbolat, "Improvement of the deformation technology in relief rolls by asymmetric rolling realization," *Ferrous Metallurgy. Bulletin of Scientific, Technical and Economic Information*, vol. 77, no. 4, pp. 445–454, 2021.

[32] A. Esbolat, E. Panin, A. Arbuz et al., "Concepts analysis of asymmetry factor implementation during rolling in relief rolls," *Journal of Chemical Technology and Metallurgy*, vol. 57, pp. 1243–1250, 2022.

[33] A. A. Bogatov and D. S. Nukhov, "Roll knot," RU Patent 156711, 2015.

[34] A. Esbolat, E. Panin, A. Arbuz et al., "Investigation of force parameters during rolling in relief rolls," *Journal of Chemical Technology and Metallurgy*, vol. 58, no. 5, pp. 961–968, 2023.